THERMODYNAMIC SCREENING OF ORGANIC RANKINE CYCLE WORKING FLUIDS AND ARCHITECTURES: APPLICATION TO AUTOMOTIVE INTERNAL COMBUSTION ENGINES

Lecompte S.*[a], Criens C.[b], Siera, I.[b], van den Broek M.[a], De Paepe M.[a]
*Author for correspondence
[a]Department of Flow, Heat and Combustion Mechanics
Ghent University,
Sint-Pietersnieuwstraat 41,
9000 Gent,
Belgium
[b]Flanders Make, Oude Diestersebaan 133, 3020 Lommel, Belgium
E-mail: steven.lecompte@ugent.be

ABSTRACT

In the presented work, three promising ORC architectures are thermodynamically investigated for application on internal combustion engines for long-haul trucks. The cycles examined are the subcritical ORC (SCORC), the partial evaporating ORC (PEROC) and the transcritical ORC (TCORC). The employed screening approach has previously been developed by the authors and is now adapted for this particular application. In total 67 working fluids are considered. Four specific cases are postulated. These include various heat source (350°C, 500°C) and heat sink (25°C, 50°C, 75°C, 100°C) conditions and two levels of maximum cycle pressure (32 bar and 50 bar). Additionally, the effect of selecting a volumetric machine as expander type is examined. The results show that the PEORC and the TCORC give the highest second law efficiencies. However, when a simple low expansion ratio volumetric expander is selected, subcritical ORCs gave the highest second law efficiencies. Furthermore methanol and ethanol, operating under subcritical conditions, give generally good results for all cases in the study.

INTRODUCTION

Organic Rankine cycles are a well-known technology for converting low-temperature heat to usable power. The associated benefits are autonomous operation, favorable operating pressures and low maintenance costs [1]. Commercial applications are typically found in solar, geothermal and industrial waste heat applications. However more emerging markets are on the horizon. Considering the current situation in the transport sector, all elements are present for a rapid adoption of ORC technology. The transport-sector accounts for a considerable fraction of the total energy use [2]: 13.5% for China, 40% for the USA, 30.4% for the EU and 29.5% worldwide. In addition, internal combustion engines (ICE) reject roughly 66% [3] of their input energy as residual heat. This heat however can be used effectively in an ORC, increasing the overall efficiency. This is crucial considering the challenges in CO_2 reduction that lie ahead. Governments worldwide are imposing stricter laws on maximum CO2 emissions requiring the need for more efficient engines in the near future [4].

For initial adoption, large scale trucks deem to be the best integration platform for waste heat recovery (WHR) technologies. These trucks reject large amounts of waste heat at a continuous rate. The large size of the system makes the technology more cost-effective, while the continuous rate of waste heat allows for an easier control. In heavy duty truck engines, the exhaust gasses typically range between 200 to 400 °C. A basic ORC directly coupled to exhaust gasses of a 130 kW combustion engine already show increased net power outputs of 2.64% to 6.96%, depending on the working fluid used [5]. Typical ORC working fluids considered in prototypes are: water [6, 7], R245fa [8] and ethanol [9]. All of the prototypes, but also most theoretical studies, are limited to the basic subcritical ORC (SCORC). Going to alternative architectures however shows potential for increased power outputs [10].

Besides the cycle architecture and the choice of working fluid, the expander is a key part of the ORC. Two types of technology are commonly used, turbines or volumetric expanders. Low power applications (2-10 kW) necessitate very high rotational speeds of turbines (>~20,000 rpm). Thus high ratio gearboxes and expensive lubrication systems are required. Leibowitz et al. [11] emphasizes the advantage volumetric machines like the double screw expander. A double screw has the benefit that relatively high rotational speeds (up to ~5,000 rpm) are possible. Thus high maximum power outputs are achievable and direct coupling to the shaft or generator is possible. For an in depth discussion on expander types and their drawbacks and benefits we refer to the comprehensive review article of Sprouse and Depcik [12]. Considering the apparent benefits of volumetric machines, these will be considered further in the following study.

In this work a thermodynamic analysis is presented for IC WHR. Besides the SCORC two alternative cycle architectures are investigated; the partial evaporating cycle (PEORC) and the transcritical cycle (TCORC). In addition, a large set of 67 working fluids are considered. Finally, the impact of choosing a volumetric expander on the thermodynamics of different cycle

architectures and the optimal working fluid choice are investigated.

NOMENCLATURE

Ė	[W/kg/s]	Exergy flow
e	[W/kg]	Specific exergy
F	[-]	Dimensionless parameter
h	[J/kg]	Enthalpy
IC		Internal combustion
PEORC		Partial evaporating ORC
PP	[°C]	Pinch point temperature difference
Q̇	[W]	Heat transfer rate
SCORC		Subcritical ORC
TCORC		Transcritical ORC
VR		Volume ratio
Ẇ	[W]	Power
WHR		Waste heat recovery
Special characters		
η	[-]	Efficiency
ε	[-]	Loss coefficient
Subscripts		
0		Dead state
I		Thermal efficiency
II		Second law effciency
c		Condenser
cf		Cold fluid stream
e		Evaporator
exp		Expander
hf		Hot fluid stream (i.e waste heat)
internal		Value internal expansion

MODELS AND OPTIMIZATION STRATEGY

Organic Rankine cycle architectures

Two alternative ORC architectures are investigated besides the SCORC; the PEORC and the TCORC. From a previous literature survey [10], these three types appear to be the most promising for waste heat recovery applications. They all share the same component layout as the basic subcritical ORC (SCORC) depicted in Figure 1. Thus cycle modifications are minimal. However their operational regime is different, as shown in the T-s diagrams of Figure 2. Their operational modifications however result in increased power output under optimal working conditions and optimal working fluid selection [13].

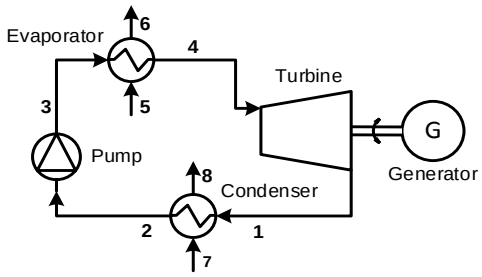

Figure 1 Component layout of the ORCs.

The basic SCORC consist of a pump which pressurizes the working fluid (3) and transports it to the evaporator. In the evaporator the working fluid is heated to the point of saturated or superheated vapour (4), cooling down the heat carrier (5-6). Next, the working fluid expands through the turbine (1) and produces mechanical work. This shaft power can then be converted to electricity or added directly to the powertrain. The superheated working fluid at the outlet of the turbine is condensed to saturated liquid (2) in the condenser by transferring the heat to a cooling loop (7-8). The liquid working fluid is again pressurized by the pump, closing the cycle. Similar to the SCORC, the TCORC consists of a pump, expander, evaporator and condenser. The working fluid is now compressed directly to supercritical pressure and heated to a supercritical state, effectively bypassing the isothermal two-phase region. Because no phase change takes place in the TCORC, the evaporator is also called a vapour generator. In contrast to the SCORC the working fluid in the PEORC is only allowed to partially evaporate. The expansion that follows is a two-phase process.

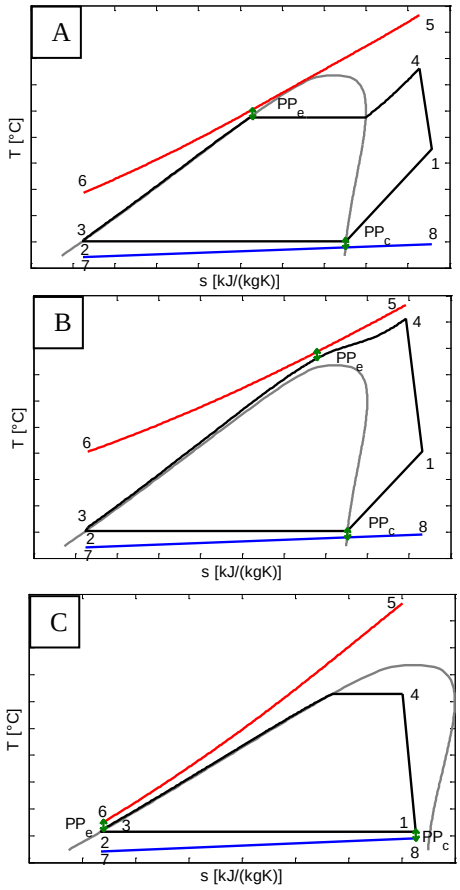

Figure 2 T-s diagram of the (a) subcritical ORC, (b) transcritical ORC and (c) partial evaporating ORC.

Model parameters

The parameters characterizing the cycles are shown in Table 1. The cycles are modelled under the assumption of steady state operation. Heat losses to the environment and pressure drops in the heat exchangers are considered negligible. A discretization approach is implemented for modelling the heat exchangers. The evaporators are segmented into $N = 20$ parts. As such, changing fluid properties are taken into account. This is particularly essential for the TCORC vapor generator. The proposed model has two degrees of freedom left. Depending on the cycle architecture these are typically defined as:

- The superheating and evaporation pressure, for the SCORC.
- The vapour quality and evaporation pressure, for the SCORC
- The turbine inlet temperature and supercritical pressure (TCORC).

In this work the independent parameters $p_{e,wf}$ and $s_{e,wf,out}$ are used as optimization parameters. These are normalized between [0 1] and given the names F_p and F_s. The benefit is that with only these two parameters the three architectures are characterized.

Table 1 ORC model parameters.

Parameter	Description	*Value*
η_{pump}	Isentropic efficiency pump [%]	70
$\eta_{\exp}$	Isentropic efficiency expander [%]	80
PP_e	Pinch point temperature difference evaporator [°C]	5
PP_c	Pinch point temperature difference condenser [°C]	5
$T_{hf,in}$	Waste heat inlet temperature [°C]	Case dependent
$T_{cf,in}$	Cooling loop inlet temperature [°C]	Case dependent
ΔT_{cf}	Cooling loop temperature rise [°C]	10
$\dot{m}_{hf}$	Mass flow rate heat carrier [kg/s]	1
$VR_{\text{int}ernal}$	Built in volume ratio [-]	5
$\varepsilon_{\exp,loss}$	Lumped loss coefficient expander [-]	0.8
$p_{e,wf}$	Evaporation pressure [bar]	Optimized
$s_{e,wf,out}$	Entropy evaporator outlet [J/kg/k]	Optimized

Two types of expander models are employed. A simple fixed isentropic efficiency model and a model that takes into account the under- and over-expansion typical for volumetric machines. This model requires the build in volume ratio ($VR_{internal}$) of the expander as an input. A typical built in volume ratio for double screw expanders is 5 [14]. The expansion process is split in an isentropic expansion and a constant volume expansion. These two are added and multiplied with a lumped loss coefficient, see Eq. 1 below.

$$\dot{W}_{\exp} = \varepsilon_{\exp,loss}\dot{m}_{wf}[(h_{\exp,in} - h_{\exp,\text{int}ernal}) + (p_{\text{int}ernal} - p_{\exp,out})VR_{\text{int}ernal}v_{\text{int}ernal}] \quad (1)$$

Optimization strategy

Each permutation of working fluid, heat source and cold source temperature is optimized over the three cycle architectures with as objective criterion maximisation of the second law efficiency (η_{II}). The second law efficiency is given as:

$$\eta_{II} = \frac{\dot{W}_{net}}{\dot{E}_{hf,in}} \quad (2)$$

The exergy flow $\dot{E}$ is obtained by multiplying the specific exergy with the mass flow rate:

$$\dot{E} = \dot{m}e \quad (3)$$

The specific exergy e for a steady state stream, assuming potential and kinetic contributions are negligible, is defined as:

$$e = h - h_0 - T_0(s - s_0) \quad (4)$$

The dead state (p_0, T_0) is defined as the inlet temperature of the condenser cooling loop.

The optimization problem is then formulated as:

$$\begin{aligned} &\max\ [\eta_{II}(x)] \\ &x = (F_s, F_p) \\ &s.t \quad 0 < F_s < 1 \\ &\qquad 0 < F_p < 1 \end{aligned} \quad (5)$$

This problem is solved with a multi-start algorithm. This is a global optimization algorithm which is partially heuristic. A uniform grid of 20 local starting points is constructed and the local solver, a trust-region algorithm [15], starts at these trail points. For more details about the modelling and optimization approach we refer to a scientific journal publication by the authors [13].

INVESTIGATED CASES

In what follows, four cases with typical values for long-haul trucks are investigated. An overview of these cases is provided in Table 2. Inlet temperatures of 350 °C (exhaust gas) and 500 °C (EGR cooling) are taken as representative values. The pressures of 32 bar and 50 bar leads to different safety levels [16]. All 67 working fluids are taken from CoolProp version 4.1.2 [17]. Removal of the non-environmentally friendly working fluids can easily be done in a post-processing step. For each case, the 15 best performing combinations of working fluid and cycle types are listed. They are ranked from high to low second law efficiency.

Table 2 Cases under investigation.

Case	Waste heat temperature (°C)	Cooling water temperature (°C)	Constraints	Expander model
I	350 & 500	25, 50, 75, 100	p_{max} < 32 bar	Fixed efficiency
II	350 & 500	25, 50, 75, 100	p_{max} < 50 bar	Fixed efficiency
III	350 & 500	25, 50, 75, 100C	VR = 5 p_{max} < 32 bar	Volumetric
IV	350 & 500	25, 50, 75, 100	VR = 5 p_{max} < 50 bar	Volumetric

Case I: Maximum pressure 32 bar, fixed isentropic efficiency

In this case, the upper pressure in the cycle is constrained to a maximum of 32 bar. The simple model of the expander is used which assumes a fixed isentropic efficiency of 0.8. First, the second law efficiency of the 15 best performing cycle/ working fluid combinations is given for a hot fluid inlet temperature of 350 °C and 500 °C in respectively Figure 3 and Figure 4. In all the following graphs, an identical scale is used when plotting the second law efficiency in order to easily discern the trends. In this case, it is clear that for increasing cold fluid inlet temperature there is a significant decrease in second law efficiency. Furthermore the second law efficiency for T_{hf} = 500 °C is consistently lower than for T_{hf} = 350 °C. A heat carrier with a higher temperature has a higher potential for doing work, however it is not possible to exploit this due to the upper pressure constraint.

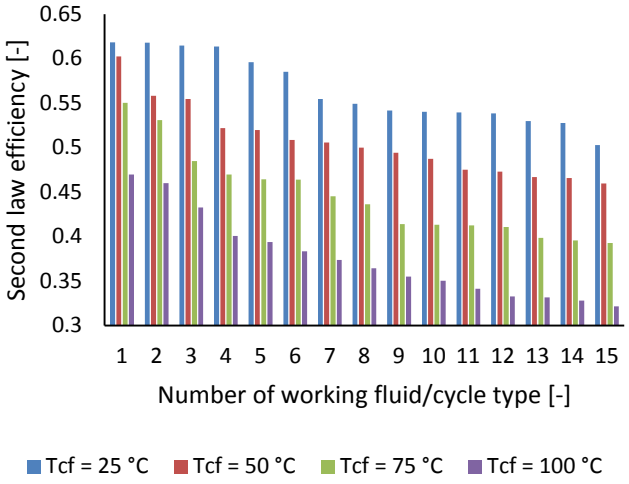

Figure 3 Second law efficiency for T_{hf} = 350 °C, Case I.

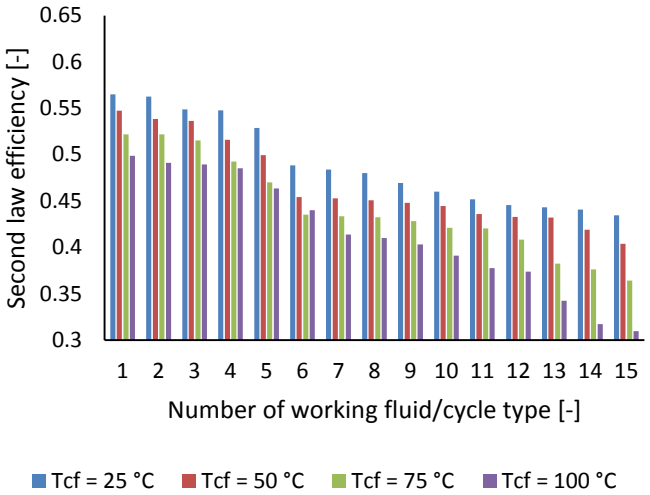

Figure 4 Second law efficiency for T_{hf} = 500 °C, Case I.

Table 3 The 15 best performing combinations of working fluid and cycle type for T_{hf} = 350 °C, Case I. (blue: SCORC, green: TCORC, red: PEORC)

cf (°C)	25	50	75	100
	Working fluid			
1	m-Xylene	Toluene	Toluene	CycloHexane
2	o-Xylene	CycloHexane	CycloHexane	Toluene
3	p-Xylene	n-Dodecane	Acetone	Acetone
4	Toluene	n-Octane	n-Heptane	Ethanol
5	n-Hexane	n-Heptane	Cyclopentane	Water
6	CycloHexane	Ethanol	Ethanol	Cyclopentane
7	n-Octane	n-Nonane	n-Hexane	n-Heptane
8	n-Decane	Cyclopentane	R113	R113
9	n-Heptane	Acetone	n-Octane	n-Hexane
10	n-Nonane	n-Hexane	Methanol	n-Octane
11	Acetone	R113	Isohexane	Methanol
12	Ethanol	m-Xylene	R141b	Isohexane
13	Cyclopentane	Methanol	R11	MM
14	n-Undecane	Isohexane	MDM	R141b
15	n-Dodecane	D4	Water	R11

Table 4 The 15 best performing combinations of working fluid and cycle type for T_{hf} = 500 °C, Case I. (blue: SCORC, green: TCORC, red: PEORC)

Tcf (°C)	25	50	75	100
	Working fluid			
1	m-Xylene	o-Xylene	p-Xylene	o-Xylene
2	p-Xylene	m-Xylene	o-Xylene	m-Xylene
3	o-Xylene	p-Xylene	m-Xylene	p-Xylene
4	Toluene	Toluene	Toluene	n-Heptane
5	Water	Water	Water	Toluene
6	Methanol	n-Undecane	n-Dodecane	Water
7	Ethanol	CycloHexane	n-Heptane	n-Dodecane
8	CycloHexane	n-Decane	n-Undecane	n-Undecane
9	n-Nonane	n-Dodecane	n-Decane	n-Decane
10	n-Octane	n-Nonane	CycloHexane	n-Nonane
11	n-Decane	n-Octane	n-Nonane	CycloHexane
12	n-Heptane	Methanol	n-Octane	n-Octane
13	Acetone	Ethanol	Acetone	Acetone
14	Cyclopentane	n-Heptane	Ethanol	D4
15	n-Dodecane	D4	Water	R11

In Table 3 and Table 4 the type of cycle and corresponding working fluid is given. The best performing cycles are typically the TCORC and the PEORC. It is approximately after the 4 best combinations of working fluid/cycle that the SCORC appears. As such, when there are no additional restrictions imposed (for example due the expander choice) alternative cycle architectures, and especially the TCORC, are beneficial to implement. Furthermore, the use of Toluene appears an interesting choice, especially under transcritical operation, due to its high performance and the fact that it is already used in ORC applications. The working fluids ethanol, methanol and water always operate under subcritical conditions. These working fluids have the benefit that they are environmentally friendly and toxicologically safe.

Case II: Maximum pressure 50 bar, fixed isentropic efficiency

Case II is almost identical to Case I except for the upper pressure constraint which is increased to 50 bar. Again, a second law efficiency plot can be found in Figure 5 and Figure 6 for respectively T_{hf} = 350°C and T_{hf} = 500 °C. Identical trends as in Case I are noticed and there is also a small performance benefit noticeable compared to Case I. Ethanol and methanol however clearly benefit when operating at increased evaporating pressures. The average increase over the different T_{cf} and T_{hf} is respectively 10.7% and 13.3%. The working fluid/cycle types are identical for both T_{hf} = 350°C and T_{hf} = 500 °C. The list can be found in Table 5. In contrast to case I all of the working fluids can go to TCORC operation for the higher waste heat inlet temperatures. Therefore no new cycle/working fluids combinations appear.

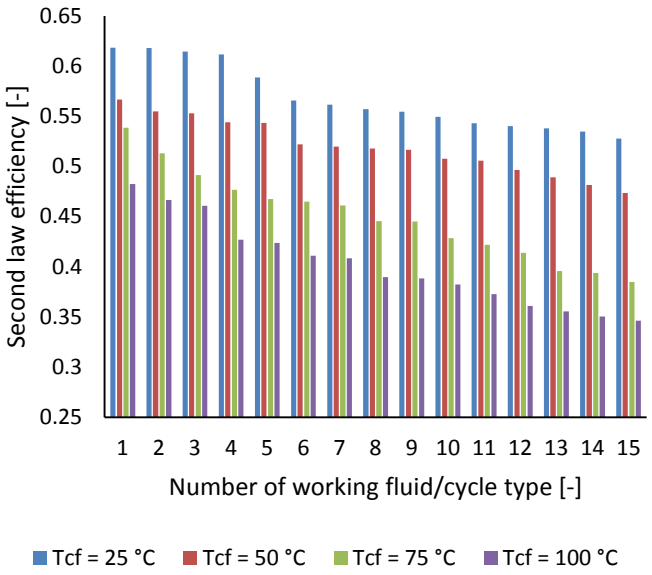

Figure 5 Second law efficiency for T_{hf} = 350 °C, Case II.

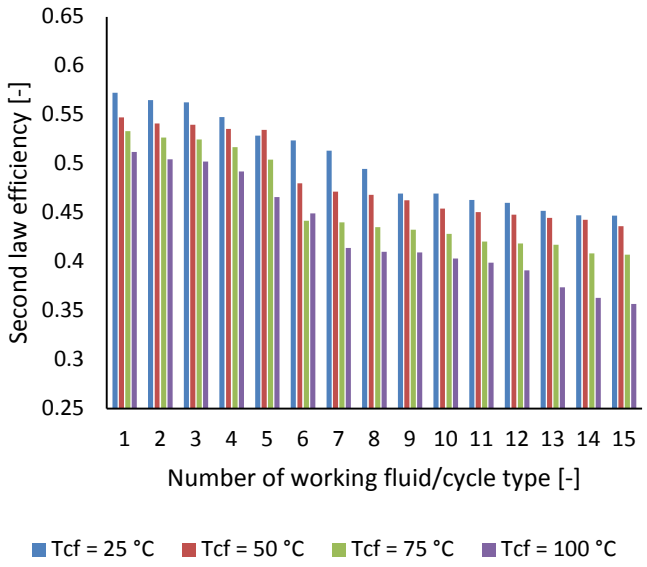

Figure 6 Second law efficiency for T_{hf} = 500 °C, Case II.

Table 5 The 15 best performing combinations of working fluid and cycle type for T_{hf} = 350 °C and T_{hf} = 500 °C , Case II. (blue: SCORC, green: TCORC, red: PEORC)

Tcf (°C)	25	50	75	100
	Working fluid			
1	m-Xylene	Acetone	Acetone	Acetone
2	o-Xylene	n-Dodecane	Ethanol	Ethanol
3	p-Xylene	CycloHexane	Cyclopentane	Methanol
4	Toluene	Cyclopentane	R11	R141b
5	CycloHexane	Ethanol	R141b	R11
6	Cyclopentane	n-Octane	CycloHexane	Cyclopentane
7	Ethanol	R11	Methanol	R113
8	Acetone	n-Heptane	n-Heptane	CycloHexane
9	n-Octane	R141b	R113	Water
10	n-Decane	R113	n-Hexane	n-Heptane
11	n-Heptane	n-Nonane	R21	n-Hexane
12	n-Nonane	n-Hexane	n-Octane	n-Pentane
13	R11	Methanol	MDM	Isohexane
14	R141b	R21	Isohexane	n-Octane
15	R113	Toluene	D4	R21

Case III: Maximum pressure 32 bar, expander model: Volume ratio =5

In Case III the model of the volumetric machine with internal built in volume ratio 5 is introduced. Also the upper pressure is limited to 32 bar. The second law efficiency is plotted in Figure 7 and Figure 8 for respectively T_{hf} = 350 °C and T_{hf} = 500 °C. Compared to the previous two cases it is immediately obvious that other trends appear. First of all, the second law efficiency is drastically lower. Secondly, the second

law efficiency now increases sometimes with increased T_{cf}. Compared to the previous cases, increasing the pressure difference by cooling to a lower condensation temperature will not result in increased second law efficiency because the volumetric expander only achieves maximum performance at a fixed volumetric ratio. Furthermore, for varying T_{cf} the second law performance remains relatively equal.

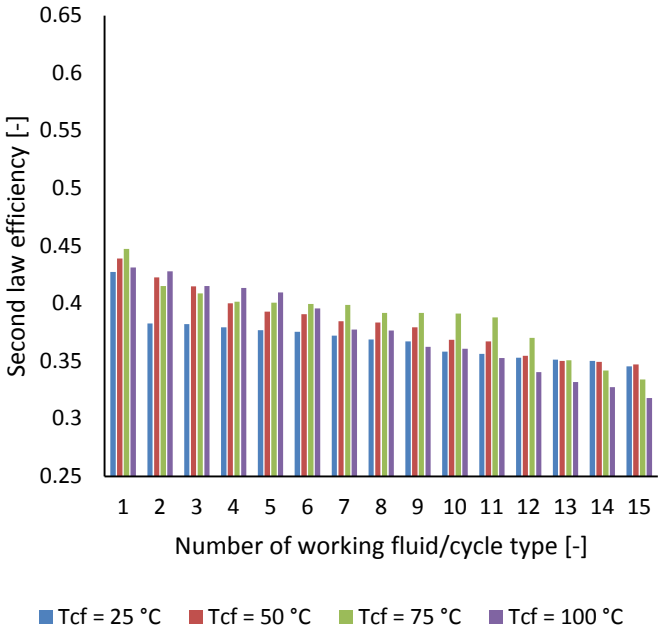

Figure 7 Second law efficiency for T_{hf} = 350 °C, Case III.

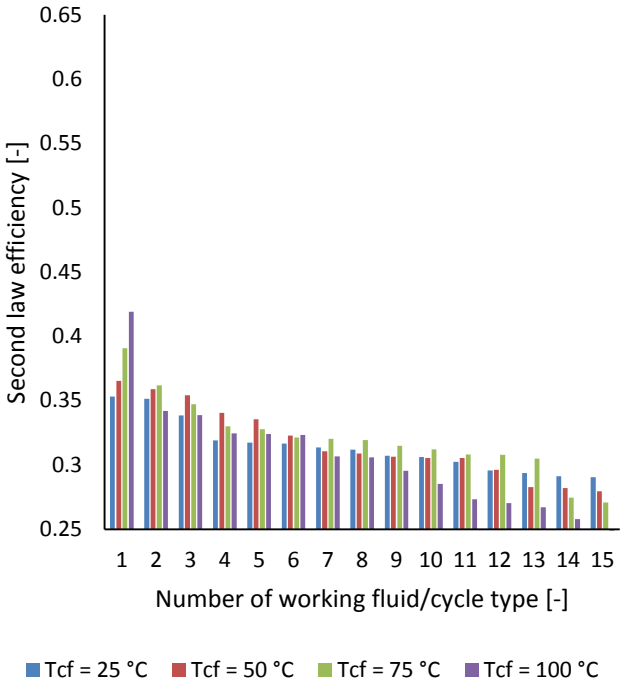

Figure 8 Second law efficiency for T_{hf} = 500 °C, Case III.

Table 6 The 15 best performing combinations of working fluid and cycle type for T_{hf} = 350 °C, Case III.
(blue: SCORC, green: TCORC, red: PEORC)

Tcf (°C)	25	50	75	100
	Working fluid			
1	R11	R11	Acetone	Acetone
2	R141b	R141b	Toluene	Toluene
3	R21	Acetone	R141b	p-Xylene
4	cis-2-Butene	Cyclopentane	CycloHexane	m-Xylene
5	Cyclopentane	R123	Methanol	o-Xylene
6	SulfurDioxide	Methanol	Cyclopentane	Ethanol
7	trans-2-Butene	R21	Ethanol	Water
8	Acetone	CycloHexane	R11	Cyclopentane
9	R1233ZDE	Toluene	p-Xylene	R113
10	Butene	R1233ZDE	m-Xylene	n-Octane
11	n-Butane	Ethanol	o-Xylene	n-Nonane
12	IsoButene	R113	R113	n-Decane
13	CycloHexane	p-Xylene	n-Heptane	Methanol
14	R113	m-Xylene	n-Octane	n-Undecane
15	R142b	cis-2-Butene	n-Pentane	n-Hexane

Table 7 The 15 best performing combinations of working fluid and cycle type for T_{hf} = 500 °C, Case III.
(blue: SCORC, green: TCORC, red: PEORC)

Tcf (°C)	25	50	75	100
	Working fluid			
1	R11	Water	Water	Water
2	SulfurDioxide	Methanol	Acetone	Acetone
3	Methanol	R11	Methanol	Toluene
4	Water	R141b	Cyclopentane	m-Xylene
5	R21	Acetone	Toluene	p-Xylene
6	R141b	Cyclopentane	R141b	o-Xylene
7	cis-2-Butene	R21	Ethanol	Cyclopentane
8	Cyclopentane	CycloHexane	R11	Ethanol
9	trans-2-Butene	Toluene	CycloHexane	CycloHexane
10	Acetone	Ethanol	R113	R113
11	R1233ZDE	R113	p-Xylene	n-Octane
12	Butene	R1233ZDE	m-Xylene	Methanol
13	n-Butane	p-Xylene	o-Xylene	n-Nonane
14	IsoButene	m-Xylene	n-Heptane	n-Decane
15	CycloHexane	n-Pentane	n-Pentane	n-Hexane

When analysing the cycle types, see Table 6 and Table 7, it is striking that the TCORC never appears on the list. This is explained by to the constraint on the maximum evaporation pressure and the low built in volume ratio of the expander. The first reason results in few working fluids which have a critical pressure lower than the maximum pressure allowed, while the second results in low performance for the TCORC.

Case IV: Maximum pressure 32 bar, expander model: Volume ratio = 5

In the last case, the maximum allowed pressure is raised to 50 bar while still using the detailed expander model with built in volume ratio of 5. From Figure 9 and Figure 10 it is clear that a small performance increase is seen compared to case III, especially for T_{hf} = 350 °C. Also the TCORC reappears. Methanol and ethanol in a SCORC are very high on the list. Both working fluids again show increased second law efficiency for higher evaporation pressure. The average increase over the different T_{cf} and T_{hf} is respectively 3.9% and 15.3%. The performance benefit for methanol due to higher pressure is mainly seen for T_{cf} = 100 °C and high T_{hf} = 500 °C.

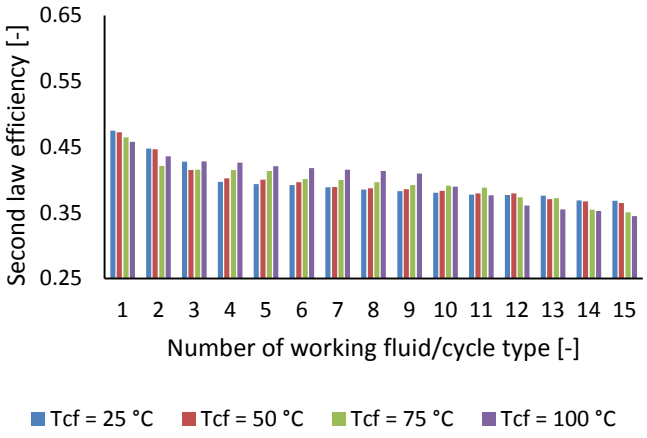

Figure 9 Second law efficiency for T_{hf} = 350 °C, Case IV.

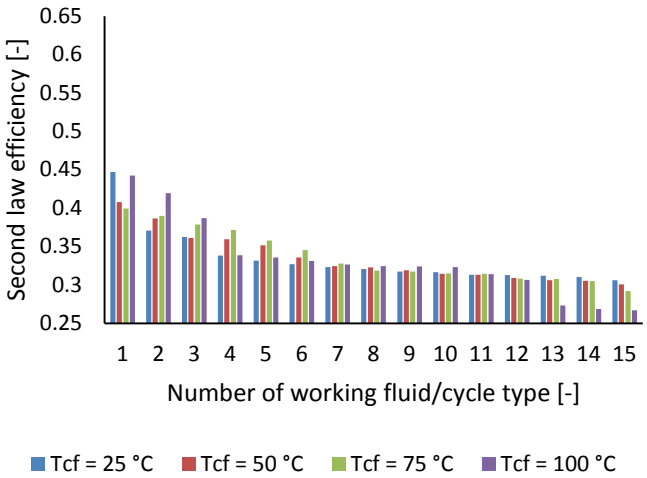

Figure 10 Second law efficiency for T_{hf} = 500 °C, Case IV.

Table 8 The 15 best performing combinations of working fluid and cycle type for T_{hf} = 350 °C, Case IV. (blue: SCORC, green: TCORC, red: PEORC)

Tcf (°C)	25	50	75	100
	Working fluid			
1	SulfurDioxide	R21	R11	Methanol
2	R21	R11	R141b	Acetone
3	R11	Acetone	Toluene	Toluene
4	cis-2-Butene	cis-2-Butene	Methanol	R141b
5	Propyne	Cyclopentane	R21	Ethanol
6	R142b	R141b	CycloHexane	R11
7	trans-2-Butene	trans-2-Butene	Acetone	p-Xylene
8	Butene	R1233ZDE	Ethanol	m-Xylene
9	R141b	R123	p-Xylene	o-Xylene
10	IsoButene	CycloHexane	m-Xylene	R113
11	R12	Toluene	o-Xylene	Cyclopentane
12	Cyclopentane	Methanol	R1233ZDE	n-Octane
13	R152A	Butene	R113	n-Pentane
14	Acetone	Ethanol	cis-2-Butene	n-Nonane
15	R1233ZDE	R142b	n-Heptane	Water

Table 9 The 15 best performing combinations of working fluid and cycle type for T_{hf} = 500 °C, Case IV. (blue: SCORC, green: TCORC, red: PEORC)

Tcf (°C)	25	50	75	100
	Working fluid			
1	SulfurDioxide	R21	Water	Methanol
2	R21	R11	R11	Water
3	R11	Water	Acetone	Acetone
4	Methanol	Methanol	Methanol	Toluene
5	Propyne	R141b	R141b	R11
6	cis-2-Butene	Acetone	R21	R141b
7	R142b	cis-2-Butene	Toluene	Ethanol
8	trans-2-Butene	Cyclopentane	Ethanol	m-Xylene
9	Butene	SulfurDioxide	Cyclopentane	p-Xylene
10	R141b	R1233ZDE	CycloHexane	o-Xylene
11	IsoButene	trans-2-Butene	R113	Cyclopentane
12	R12	CycloHexane	p-Xylene	R113
13	Cyclopentane	Toluene	m-Xylene	n-Octane
14	R152A	Ethanol	o-Xylene	n-Pentane
15	Acetone	R113	R1233ZDE	n-Nonane

CONCLUSION

A screening approach for ORCs was performed specifically focused on the constraints of automotive internal engines. Four specific cases with typical values for long-haul trucks have been investigated. From these cases several interesting conclusions could be drawn:

- Model expander: fixed isentropic efficiency.
  - Alternative cycle architectures and especially the transcritical ORC appear promising.
  - The cold sink temperature has a large influence on the second law efficiency. For increased cold sink temperature the second law efficiency decreases almost linearly.
  - When putting constraints on the evaporation pressure and increasing the hot source temperature, the second law efficiency decreases. A heat carrier with a higher temperature has a higher potential for doing work, however it is not possible to exploit this due to the upper pressure constraint.
  - Ethanol and methanol benefit with working at an evaporation pressure of 50 bar instead of 32 bar. The average increase over the different hot source and cold sink temperatures is respectively 10.7% and 13.3%.
- Model expander: fixed built in volume ratio.
  - The second law efficiency is drastically decreased due to the low built in volume ratio.
  - Increasing cold sink temperature does not automatically result in reduced second law efficiency due to the fact that there is an optimal operational volume ratio over the expander that should match the built in volume ratio.
  - The transcritical ORC does not appear in the list of best performing cycle/working fluid combinations when limiting the maximum evaporation pressure to 32 bar. When constraining the upper pressure to 50 bar the TCORC reappears. However, the SCORC always gives the highest second law efficiency.
  - Methanol and ethanol in a SCORC are promising choices.
  - There is now only a small performance benefit when going to higher pressures for the ethanol and methanol. The average increase over the different T_{cf} and T_{hf} is respectively 3.9% and 15.3%. The performance benefit for methanol due to higher pressure is however mainly seen for T_{cf} = 100 °C and high T_{hf} = 500 °C.

REFERENCES

[1] B.F. Tchanche, G. Lambrinos, A. Frangoudakis, G. Papadakis. Low-grade heat conversion into power using organic Rankine cycles – A review of various applications Renewable and Sustainable Energy Reviews 15 (2011) 3963 - 79.

[2] S. Jia, H. Peng, S. Liu, X. Zhang. Review of Transportation and Energy Consumption Related Research. Journal of Transportation Systems Engineering and Information Technology. 9 (2009) 6-16.

[3] W. Lang, P. Colonna, R. Almbauer. Assessment of Waste Heat Recovery From a Heavy-Duty Truck Engine by Means of an ORC Turbogenerator. Journal of Engineering for Gas Turbines and Power. 135 (2013) 042313-.

[4] D. Streimikiene, T. Baležentis, L. Baležentienė. Comparative assessment of road transport technologies. Renewable and Sustainable Energy Reviews. 20 (2013) 611-8.

[5] A. Domingues, H. Santos, M. Costa. Analysis of vehicle exhaust waste heat recovery potential using a Rankine cycle. Energy. 49 (2013) 71-85.

[6] I. Ibaraki, T. Endo, Y. Kojim, K. Takahashi, T. Baba, S. Kawajiri. Study of efficient on-board waste heat recovery system using rankine cycle. Review of Automotive Engineering. 28 (2007) 307-13.

[7] R. Freymann, W. Strobl, A. Obieglo. The turbosteamer: A system introducing the principle of cogeneration in automotive applications. MTZ worldwide. 69 20-7.

[8] C.R. Nelson. APPLICATION OF REFRIGERANT WORKING FLUIDS FOR MOBILE ORGANIC RANKINE CYCLES. 3rd International Seminar on ORC Power Systems, Brussels, 2015.

[9] J. Galindo, V. Dolz, L. Royo, R. Haller, J. Melis. STUDY OF A VOLUMETRIC EXPANDER SUITABLE FOR WASTE HEAT RECOVERY FROM AN AUTOMOTIVE IC ENGINE USING AN ORC WITH ETHANOL 3rd International Seminar on ORC Power Systems2016.

[10] S. Lecompte, H. Huisseune, M. van den Broek, B. Vanslambrouck, M. De Paepe. Review of organic Rankine cycle (ORC) architectures for waste heat recovery. Renewable and Sustainable Energy Reviews. 47 (2015) 448-61.

[11] H. Leibowitz, I.K. Smith, N. Stosic. Cost Effective Small Scale ORC Systems for Power Recovery From Low Grade Heat Sources. ASME 2006 International Mechanical Engineering Congress and Exposition, Chicago, USA, 2006.

[12] C. Sprouse Iii, C. Depcik. Review of organic Rankine cycles for internal combustion engine exhaust waste heat recovery. Applied Thermal Engineering. 51 (2013) 711-22.

[13] S. Lecompte, H. Huisseune, M. van den Broek, M. De Paepe. Methodical thermodynamic analysis and regression models of organic Rankine cycle architectures for waste heat recovery. Energy. 87 (2015) 60-76.

[14] V. Lemort, L. Guillaume, A. Legros, S. Declaye, S. Quoilin. A comparison of piston, screw and scroll expanders for small scale Rankine cycle systems. Proceedings of the 3rd International Conference on Microgeneration and Related Technologies2013.

[15] R.H. Byrd, J.C. Gilbert, J. Nocedal. A trust region method based on interior point techniques for nonlinear programming. Mathematical Programming. 89 (2000) 149-85.

[16] European Union. DIRECTIVE 2014/68/EU. 2014.

[17] I.H. Bell, J. Wronski, S. Quoilin, V. Lemort. Pure and Pseudo-pure Fluid Thermophysical Property Evaluation and The Open-Source Thermophysical Property Library Coolprop. Industrial & Engineering Chemistry Research. 53 (2014) 2498-508.